General Disclaimer

One or more of the Following Statements may affect this Document

- This document has been reproduced from the best copy furnished by the organizational source. It is being released in the interest of making available as much information as possible.

- This document may contain data, which exceeds the sheet parameters. It was furnished in this condition by the organizational source and is the best copy available.

- This document may contain tone-on-tone or color graphs, charts and/or pictures, which have been reproduced in black and white.

- This document is paginated as submitted by the original source.

- Portions of this document are not fully legible due to the historical nature of some of the material. However, it is the best reproduction available from the original submission.

X-953-77-239
PREPRINT

TMX 71412

MONTE CARLO SIMULATION OF WAVE SENSING WITH A SHORT PULSE RADAR

D. M. LE VINE
L. D. DAVISSON
R. L. KUTZ

OCTOBER 1977

GSFC — GODDARD SPACE FLIGHT CENTER —
GREENBELT, MARYLAND

X-953-77-239

MONTE CARLO SIMULATION OF WAVE SENSING WITH A SHORT PULSE RADAR

D. M. Le Vine
Goddard Space Flight Center

L. D. Davisson
University of Maryland

R. L. Kutz
Goddard Space Flight Center

October 1977

GODDARD SPACE FLIGHT CENTER
Greenbelt, Maryland

MONTE CARLO SIMULATION OF WAVE SENSING WITH A SHORT PULSE RADAR

D. M. Le Vine
Goddard Space Flight Center

L. D. Davisson
University of Maryland

R. L. Kutz
Goddard Space Flight Center

ABSTRACT

A Monte Carlo simulation has been developed for the scattering of short pulses from corrugated stochastic surfaces using a physical optics analysis for the scattering. The simulation has been used to study the ocean wave sensing potential of a radar which scatters short pulses at small off-nadir angles and a comparison with experiments has been made. In the simulation, realizations of a random surface are created commensurate with an assigned probability density and power spectrum. Then the signal scattered back to the radar is computed for each realization using a physical optics analysis which takes wavefront curvature and finite radar-to-surface distance into account. In the case of a Pierson-Moskowitz spectrum and a normally distributed surface, reasonable assumptions for a fully developed sea, it has been found that the cumulative distribution of time intervals between peaks in the scattered power provides a measure of surface roughness. This observation is supported by experiments.

CONTENTS

	Page
ABSTRACT	iii
INTRODUCTION	1
SIMULATION	5
RESULTS	12
ACKNOWLEDGMENT	17
REFERENCES	18

ILLUSTRATIONS

Figure		Page
1	The Short Pulse Radar Concept	1
2	Example of the scatter due to a single transmitted pulse. This data was obtained on September 30, 1976 in the vicinity of hurricane Gloria. The radar was aboard the NASA CV-990 at an altitude of approximately 9 km and the antenna (a printed circuit antenna) pointed at 10° from nadir.	3
3	Examples of simulated surfaces. The surfaces have been assumed to be normally distributed and fully developed with a Pierson-Moskowitz spectrum. U is the wind speed to which the surface corresponds.	7
4	Examples of the simulated radar signal. On the right is an example of the simulated radar return due to a single transmitted pulse and on the left is shown the average of 4096 such signals.	9
5	Comparison of simulated data and measured radar return. The measured data were obtained during JONSWAP-75.	10
6	Cumulative distribution of time intervals between peaks in the scatter by a single pulse. These curves represent simulated data using surfaces corresponding to wind speeds of 6, 10, and 20 M/s.	13

ILLUSTRATIONS (Continued)

Figure		Page
7	Flight Line Along Which Data was Collected During JONSWAP-75	15
8	Cumulative Distribution of Interval Between Peaks Using Data Obtained During JONSWAP-75	16

MONTE CARLO SIMULATION OF WAVE SENSING WITH A SHORT PULSE RADAR

INTRODUCTION

For several years now the Goddard Space Flight Center has been developing a short pulse radar system for measuring ocean waves. This is a versatile system, employing a real aperture radar, which has the potential for making several surface measurements. The GSFC system transmits a very short pulse of microwave radiation providing intrinsic resolution in range, and employs the antenna aperture to obtain resolution in azimuth. The bandwidth inherent in the short pulse permits (in principle) the digital recreation of many of the active sensor measurements which have been promulgated for ocean applications. In addition to its potential for wave monitoring in a near nadir mode, the short pulse radar can operate in a scatterometer mode to obtain local wind speed and in an altimeter mode to determine sea state. It has also been used in an imaging mode employing a real aperture antenna, and what it lacks in this mode in potential resolution (e.g., compared to a synthetic aperture radar) it makes up in wide swath coverage, simplicity, and relatively low data rates. The short pulse radar has also been operated over ice and snow to test its potential to provide information on roughness for such surfaces.

The concept of the short pulse radar for surface measurements is illustrated in Figure 1. The sensor radiates a pulse of microwave radiation τ seconds long (about 10 ns in the prototype system currently in existence) from an antenna with a beam width of θ_B degrees and pointing at θ_N degrees from nadir. The beam

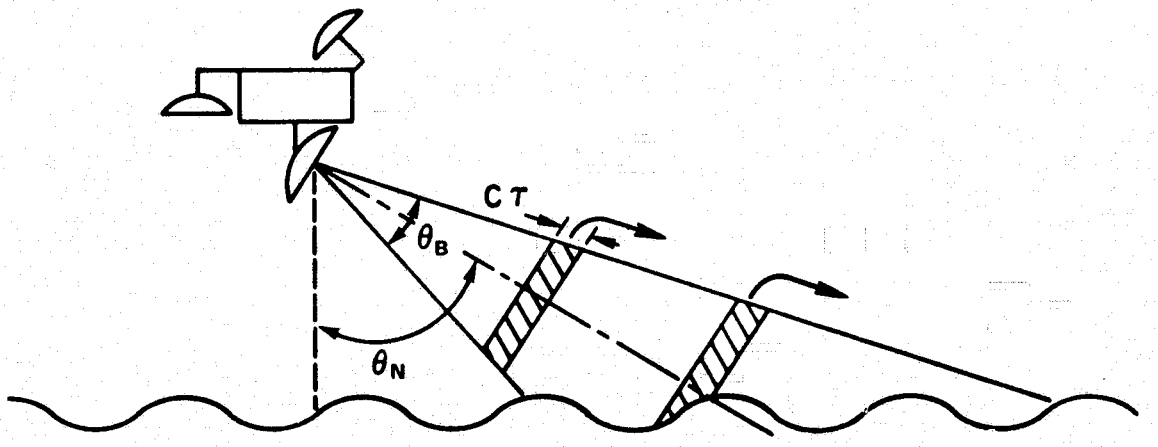

Figure 1. The Short Pulse Radar Concept

width perpendicular to the figure is made much smaller than θ_B by design of the physical dimensions of the antenna. As a result, the illuminated footprint on the surface is a long narrow, "pencil" beam. When the pulse reaches the surface it intersects a length $c\tau/\sin\theta$ on the mean surface where θ is the local angle of incidence measured relative to the mean surface. As the pulse propagates this intersection moves across the footprint. If $c\tau/\sin\theta$ is smaller than the wavelength of the dominant wave mode on the surface, then the pulse intersects the actual surface at different local angles as it moves across the footprint, and a corresponding modulation of the scattered power is to be expected. (An example of data collected during a recent CV-990 flight is shown in Figure 2. The figure represents the signal scattered back to the radar by a single transmitted pulse.) .

The precise manner in which the surface modulates the scattered signal depends on the physics of the interaction of short pulses of microwave energy with rough surfaces. Although this is still an area of active research, many of the general characteristics of the scatter are understood (Barrick, 1972; Barrick and Peake, 1968; Bass, et al., 1968). For example, if the sensor points at nadir (altimeter mode), the interaction results in a broadening of the leading edge of the pulse (actually a convolution with the characteristic function of surface height) which can be used to infer sea state (significant wave height). Alternatively, when θ_N is greater than about 20° the scatter is primarily resonant (Bragg) scatter from the capillary and small gravity waves possibly modulated by the longer gravity waves. Since the capillaries are responsive to local winds, one has in this "scatterometer" mode, a potential for monitoring winds; and to the extent that one can identify the modulation due to the long gravity waves, a potential for information on the gravity wave spectrum (Harger and Le Vine, 1976). In the case of small but non-zero θ_N (near nadir mode) the dominant scatter mechanism is specular scatter from the gravity waves. Scatter in this regime may provide information on both sea state and direction of the gravity waves.

The short pulse radar, could be the central ingredient in a multiple purpose oceanographic radar system for spacecraft use. Such a system would consist of a single radar with several antennas pointing in different directions. These antennas would include a nadir horn for sea state monitoring and ice profiling and a compliment of pencil beam antennas with footprints ranging from near nadir to large off-nadir angles. These antennas would give directional information on surface structure such as winds and waves. The system could provide most of the active oceanographic measurements currently planned for Seasat in the open ocean and in addition provide large swath coverage in each pass of the spacecraft.

As part of the analytical work being performed in support of the radar program, a simulation has been developed for the near nadir scatter of short pulses from corrugated surfaces. The simulation was undertaken to help determine how the

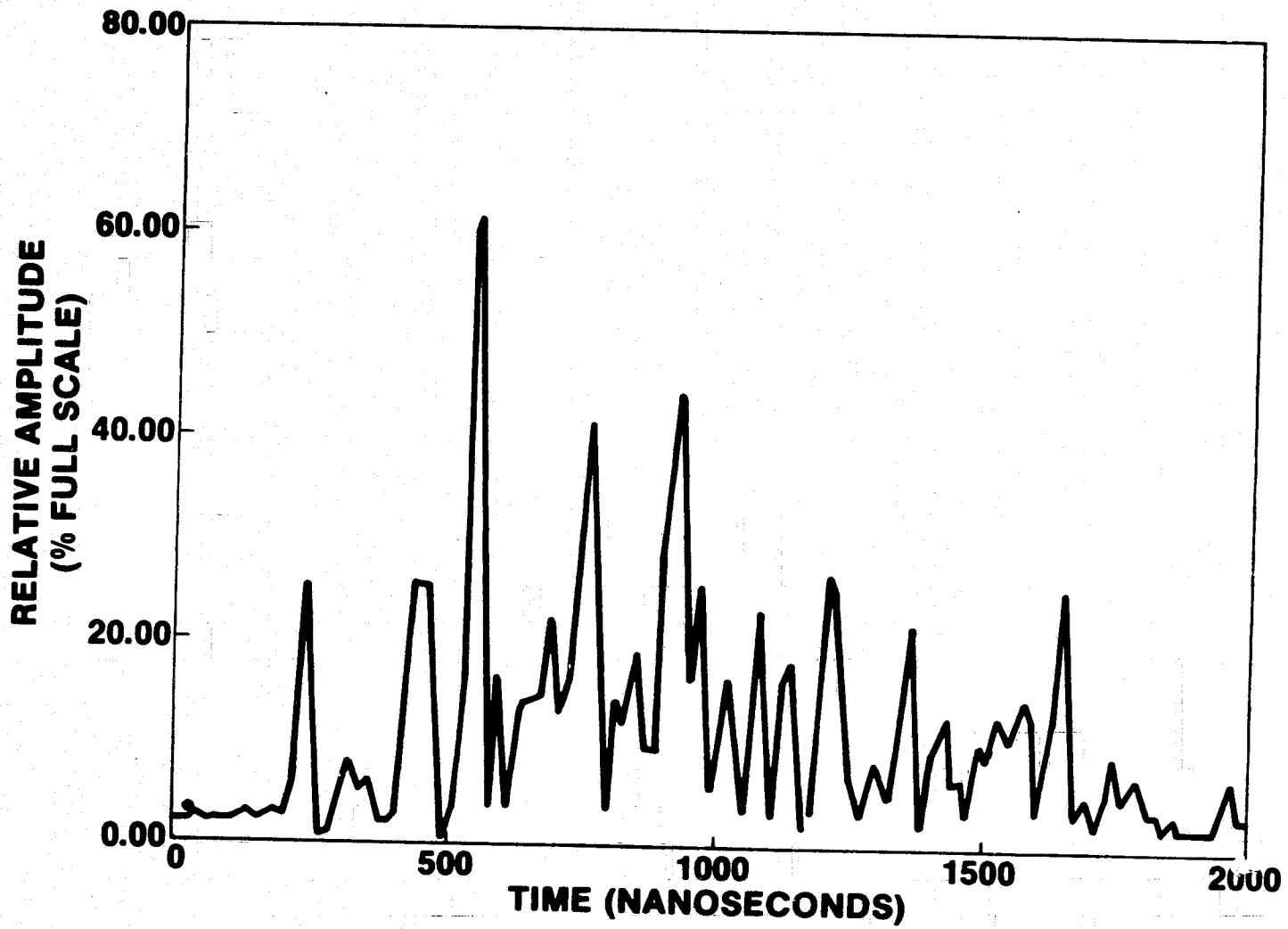

Figure 2. Example of the scatter due to a single transmitted pulse. This data was obtained on September 30, 1976 in the vicinity of hurricane Gloria. The radar was aboard the NASA CV-990 at an altitude of approximately 9 km and the antenna (a printed circuit antenna) pointed at 10° from nadir.

scattered signal is related to surface parameters. In particular, an objective of the simulation was to determine whether or not the time between peaks in the scattered power could be related to wave structure, as suggested in an earlier analysis (Le Vine, 1974). Simulated data were created in the two dimensional case (corrugated surfaces) and examined for a dependence on sea state. It was found that the cumulative distribution of the time interval between peaks is a function of sea state; and corroborating experimental evidence was found in the data obtained with the GSFC radar during JONSWAP-75 (Le Vine, et al., 1977). The purpose of this report is to describe the simulation and these results.

SIMULATION

The simulation consists of two parts: A computer routine for generating realizations of the stochastic surface, and a solution of the electromagnetic problem for the scattering of short pulses from a given realization.

The electromagnetic problem has been solved in two dimensions (i.e., line sources above corrugated surfaces) in the special case of backscatter from a perfectly conducting surface. This is an idealized model relevant in first order for scattering from ocean surfaces and to some extent for scattering from plowed fields and perhaps ice. The restriction to two dimensions has been chosen for the obvious simplification in treating the vector problem. A physical optics solution is obtained for this geometry and is reasonable for microwave radar scattering near nadir, at least for ocean surfaces (Bass, et al., 1968; Barrick, 1968a-b). This solution has been formulated here to include both the effects of the antennas and finite nature of the source. This has been done by first representing the antenna used for transmission with an equivalent distribution of current. This reduces the electromagnetic problem on transmission to an inhomogeneous wave equation which must be solved commensurate with the boundary conditions on the (random) surface. A formal solution for the scattered portion of the fields can be obtained in the form of a Helmholtz integral over the boundary. However, the integrand involves the fields on the surface, which are unknown functions. A common procedure for evaluating this integral, and the one used here, is to use the Kirchoff approximation to specify the unknown functions and then to evaluate the remaining integral asymptotically in the limit of high frequency. The result is a physical optics solution for the fields scattered back to the source but in this case in a form which includes explicitly the radiation pattern of the antenna and the curvature of the incident phase fronts. The expression for the scattered fields which is obtained in this manner is then weighted by a transfer function (the effective area) to account for the receiving antenna. The result is the signal available to be processed by the radar. This signal has the following form in the time domain (Le Vine, 1977):

$$E(t) = E_o \sum_{\text{all } n} \frac{G(y_n)}{2\pi R(y_n)} \left[\left| \frac{R_c(y_n)}{1 - R_c(y_n)/R(y_n)} \right| \right]^{1/2} F\left(t - \frac{2R(y_n)}{C} \right) \qquad (1)$$

where the summation is over all the stationary points, y_n, and where $R(y_n)$ is the distance from the source to the n-th stationary point on the surface, $R_c(y_n)$ is the radius of curvature of the surface at this point, F(t) is the transmitted pulse, and $G(y_n)$ is the antenna's (power) pattern in the direction of the n-th stationary point (assuming identical antennas for transmitting and receiving). E_o is a constant.

E(t) in Equation (1) is the signal into the radar's processor. The processor is also modeled in the simulation. The detector is assumed to be a simple envelope detector, a reasonable model for the actual radar which is incoherent. In this case the signal out of the detector is just the magnitude of E(t) in Equation (1). (The actual radar is chirped; however, the chirp and compression processes are well enough matched that the compressed pulse is a reasonable approximation to the original input pulse.) In order to store the data obtained during JONSWAP-75, the signal out of the radar was sampled (at a rate of about once every 10 ns) and stored. To make sure that the effects of the sampling on the reconstructed data are included in the simulation, the simulated data are also sampled (at a 100 MHz rate). The sampled data is the final product of the simulation.

In order to obtain the radar output from Equation (1), one needs to specify the surface. For purposes of the simulation, it is assumed that the surface, Z(x), is a stationary, Gaussian random process with a Pierson-Moskowitz power spectrum:

$$S_z(k) = \frac{a}{k^3} e^{-b/k^2} \qquad (2)$$

where $a = 8.1 \times 10^{-3}$ and $b = 0.74[g^2/U^4]$ and g is acceleration of gravity, U is the wind speed, and $k = 2\pi/\lambda$ is the wave number associated with each spectral component. These are reasonable hypotheses for a fully developed sea (Barrick, 1972; Pierson and Moskowitz, 1964). The realizations are created first in wave number (i.e., k) space and then transformed by means of a fast Fourier transform to coordinate space. Given a desired spatial resolution, Δx, and number of points, N, one generates N unit normal (Gaussian) independent random variables, g_n. Since $\Delta k \Delta x = 1/N$, the required interval in k-space is determined and one computes independent random variables, $F_n(n\Delta k) = \sqrt{S_z(n\Delta k)}\, g_n$, whose variance is $S_z(n\Delta k)$. A particular choice of the F_n determines the realization in k-space, and then a fast Fourier transform produces the realization at each of the desired points in x-space. Several examples of the surface simulated in this manner are shown in Figure 3.

For purposes of evaluating the scattered fields both the first and second derivatives of the realization are also required (to determine the location of the stationary points and the radius of curvature of the surface at these points). These are obtained as above, first in k-space taking advantage of the assumed stationarity of the process to form spectra from $S_z(k)$ for each derivative (i.e., $k^2 S_z(k)$ and $k^4 S_z(k)$), and then transforming to coordinate space. However, a problem is encountered in doing this, because the spectrum $k^4 S_z(k)$ for the second derivative is not bounded at large k and even $k^2 S_z(k)$ is not integrable over the interval $0 \leqslant k \leqslant \infty$. This problem has been handled here by arbitrarily

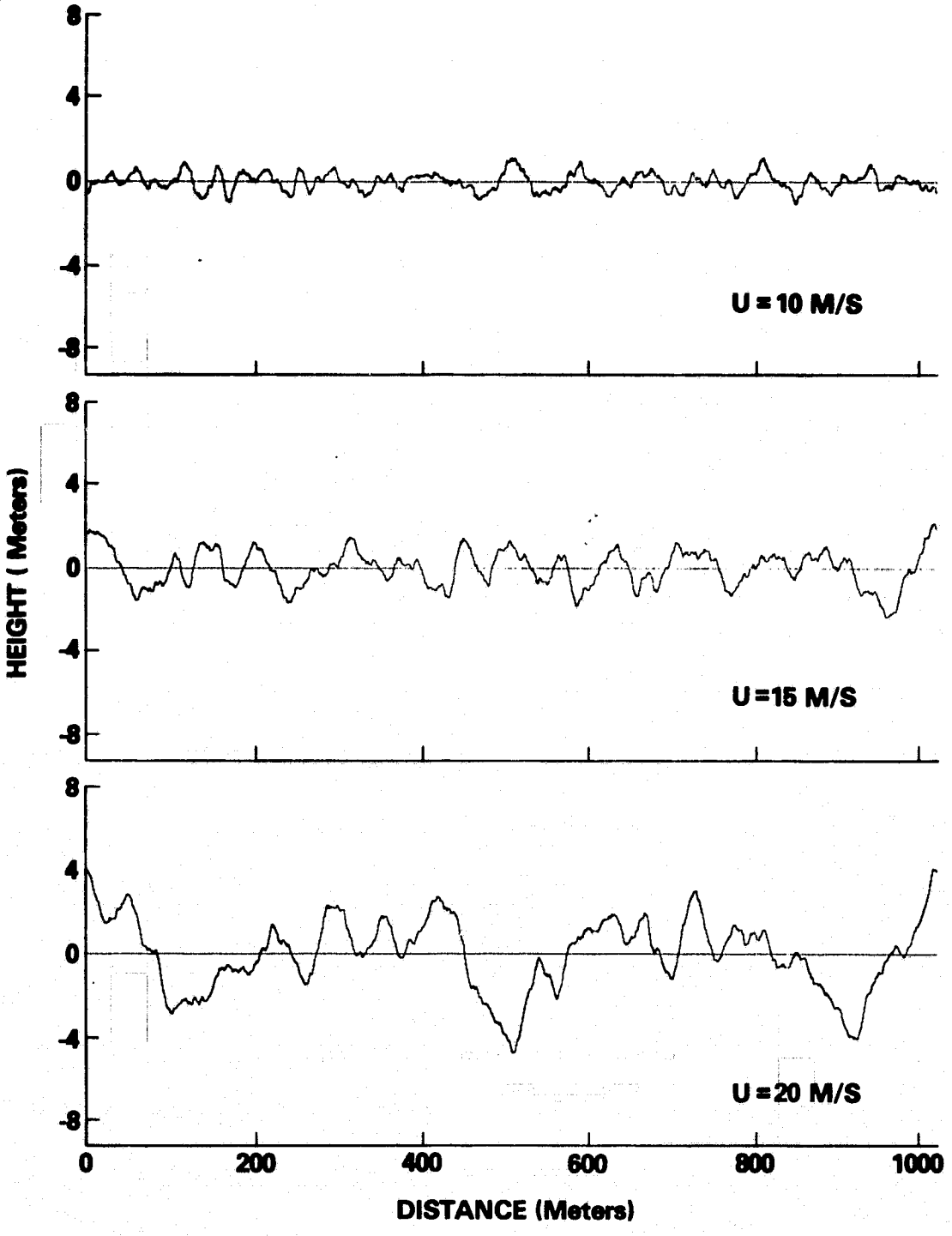

Figure 3. Examples of simulated surfaces. The surfaces have been assumed to be normally distributed and fully developed with a Pierson-Moskowitz spectrum. U is the wind speed to which the surface corresponds.

terminating the spectra at $k = 1m^{-1}$; however, this is not entirely satisfactory since the value at which the spectrum is terminated is arbitrary in the present formulation. This is a point requiring further attention.

In order to obtain an expression for the received signal from Equation (1), one needs in addition to the surface, a model for the antenna (to determine G(y)) and for the transmitted pulse, F(t). For this purpose the field pattern of the "stick" antennas used during JONSWAP-75 (Le Vine, et al., 1977) was used in the simulation. These antennas have a $(\sin x/x)^2$ main lobe roughly 26° wide and were operated for the most part with the beam center pointing at 18° from nadir. These parameters determine G(y) in Equation (1) and with the altitude of the observation (roughly 2 km during JONSWAP-75) determine the footprint on the surface and R(y). For purposes of the simulation, the pulse shape, F(t), is assumed to be a Gaussian shaped pulse 6 ns wide (i.e., $\sigma = 6$ ns), which is reasonable for the radar used during JONSWAP-75.

An example of the simulated signal is shown in Figure 4. Both a simulation of scatter by a single pulse and the average over several thousand pulses (4096 pulses) is shown. These results were obtained assuming the radar to be at 2 km above a fully developed surface generated by a 10m/s wind. (U = 10m/s in Eq. (2).)

The simulated data are in reasonable agreement with actual data collected by the radar. A comparison using data obtained during JONSWAP-75 is shown in Figure 5. The JONSWAP data presented in the figure were obtained using a horizontally polarized (E-plane) stick antenna pointing at 18° from normal. The aircraft was at about 2 km altitude and the data presented here were obtained during the morning of September 9, 1977. (See Le Vine, et al., 1977.) Winds for this period were estimated at about 10 m/s and preliminary wave rider spectra indicate nearly fully developed seas. An example of the return from a single pulse (right) and the average over 1500 pulses (left) are shown. The simulated date correspond to a comparable geometry (antenna pointing at 18°, 2 km altitude and a beam shape approximately that of the E-plane stick) and fully developed seas produced by 10m/s winds. The simulated data were sampled at once every 10 ns just as in the actual data and employed a Gaussian pulse 6 ns wide ($\sigma = 6$ ns), also representing the actual system. Both an example of the simulated return from a single pulse and the return averaged over 4096 pulses are shown.

As can be seen in Figure 5, the agreement between simulation and actual data is reasonable; however, differences are apparent especially in the case of the average return. The examples of JONSWAP data shown here are typical of real data. In particular the average data are relatively smooth and certainly don't show the large peaks apparent in the simulated results (e.g., at about 300 ns). This may be due to the very large (in fact, unbounded) signals which can occur in the

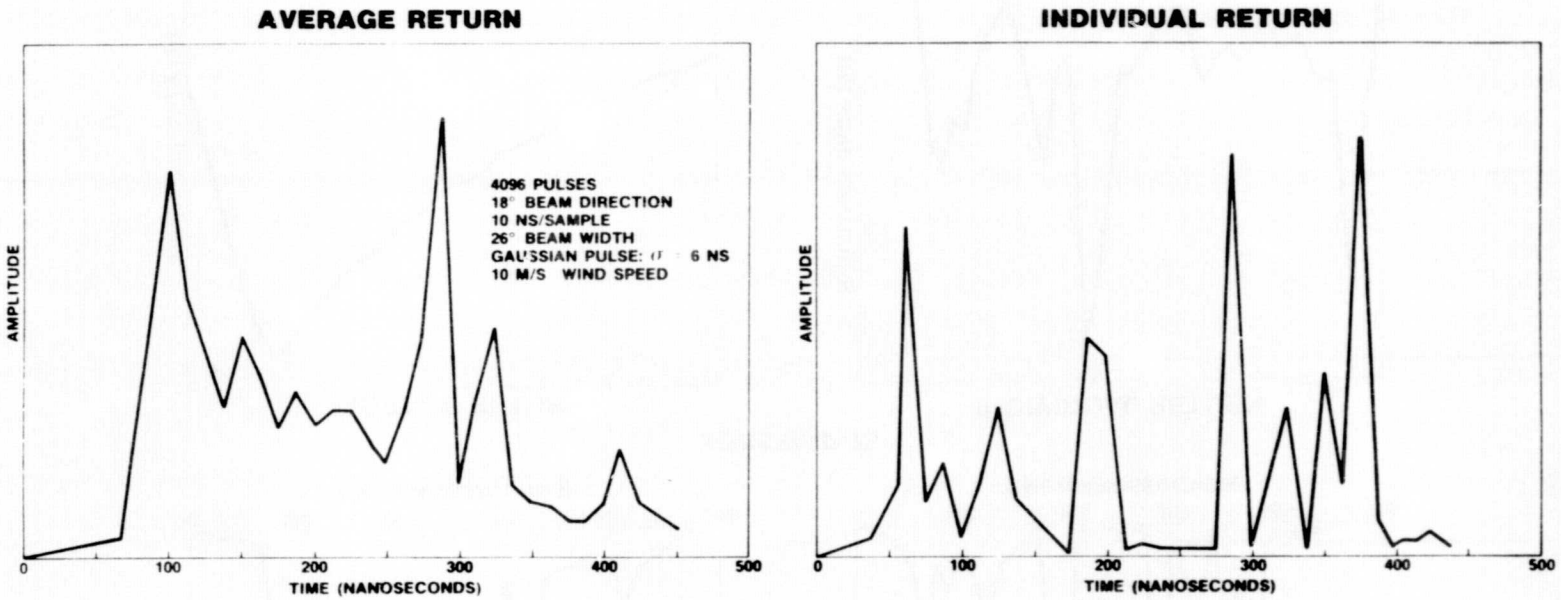

Figure 4. Examples of the simulated radar signal. On the right is an example of the simulated radar return due to a single transmitted pulse and on the left is shown the average of 4096 such signals.

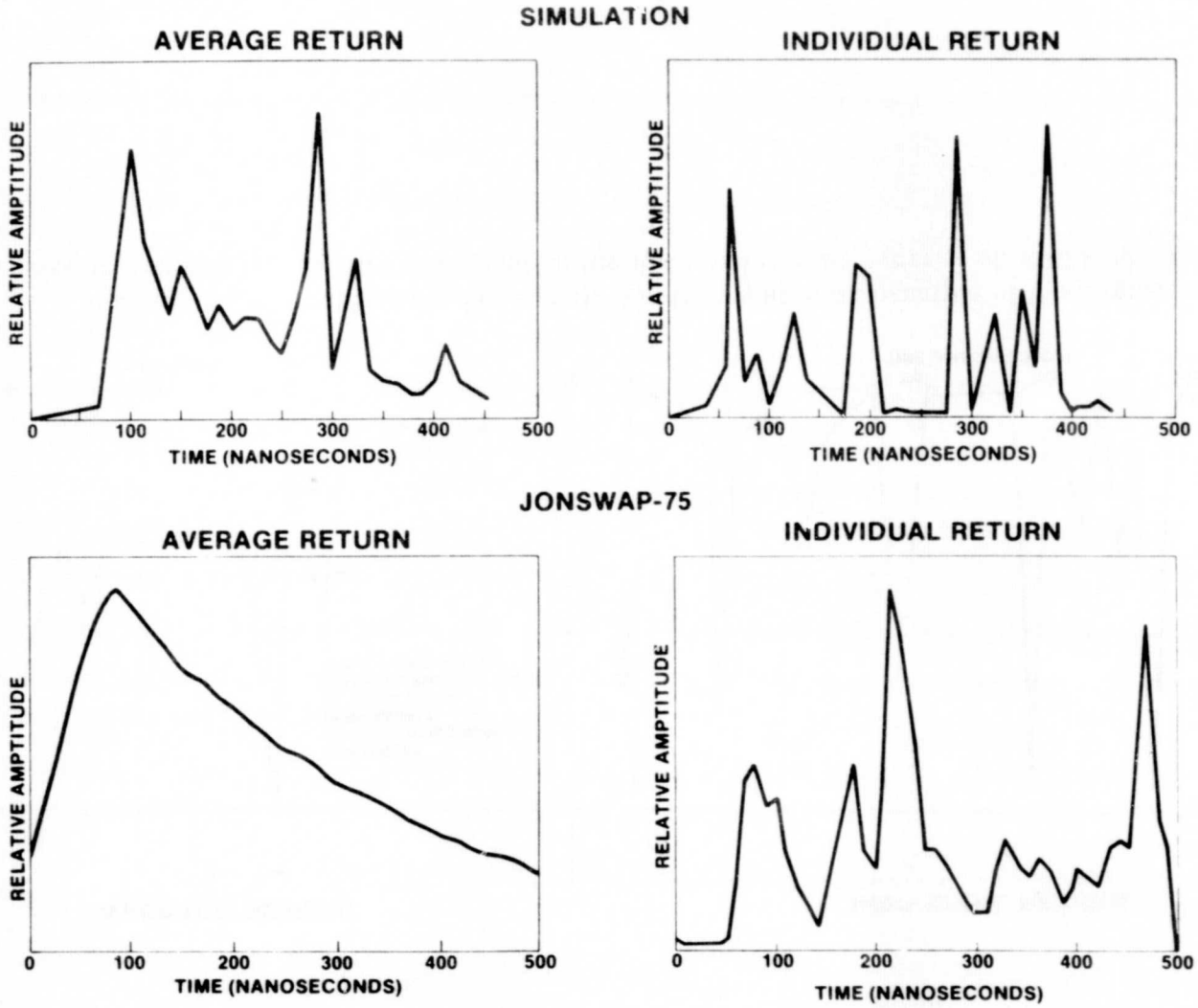

Figure 5. Comparison of simulated data and measured radar return. The measured data were obtained during JONSWAP-75.

simulated results; such signals don't occur in the actual data because the dynamic range of the radar effectively limits the maximum signal which can be recorded. However, large amplitude signals, even if only occurring infrequently in the simulation, can dominate the average. On the other hand, the smoothness of the actual data might be the result of azimuthal averaging (i.e., the effect of the third dimension) or the effect of the finite crest length of real ocean waves, effects not included in the (two dimensional) simulation. These are effects which are being investigated.

RESULTS

Intuition based on a physical optics analysis suggests that it may be possible to obtain information on gravity waves from the time between the peaks in the received signal. To understand this, imagine a simple surface with one stationary point per wave. In the physical optics solution, each stationary point scatters a single pulse identical to the transmitted pulse; hence, by making the transmitted pulse short enough, one receives a well defined pulse from each stationary point. Assuming that each stationary point occurs at the same height above the mean surface, a straightforward exercise in trigonometry relates the time between pulses to the distance between stationary points and therefore to the distance between waves. The case of real ocean surfaces is similar but more complex because of its description as a random process. In such a case the concept of a wave is only meaningful in a stochastic sense and the occurrence of stationary points is also stochastic. Also in the case of real surfaces the stationary points don't occur at the same height above the mean surface, so that the time interval between pulses depends on both the horizontal and vertical distance between stationary points. Furthermore, with realistic surfaces the stationary points may occur close enough together that individual pulses can't be distinguished. Nevertheless, it may be possible to relate the statistics of the time interval between pulse to statistics of the surface even when no relationship can be established for individual pulses.

This intuition was tested with the simulation and in fact is verified in the simulated data. An example is shown in Figure 6 where the cumulative distribution of the interval between power peaks obtained with the simulated data is plotted for several surfaces. In Figure 6 the cumulative distribution for pulse intervals has been plotted in terms of equivalent distance on the mean surface. A given time interval between received pulses can be related to a distance between hypothetical scatterers on the mean surface given the location of the receiver and the nominal direction from which the pulses scatter, things which are known in the simulation and are generally known in measured data. This conversion has been made in the data presented in Figure 6. This has been done for surfaces corresponding to winds of 6, 10 and 20 m/s, and assuming that the radar is at an altitude of 2 km with the antenna pointing at 18° from the normal. As can be seen from the simulated data, as the wind speed increases (i.e., for higher and higher seas) the distribution of power peaks shifts toward longer intervals between pulses. This is what one would expect for waves since the mean wavelength of the ocean waves is also increasing as the seas become rougher.

Data obtained with the GSFC shoft pulse radar corroborates the dependence on sea state demonstrated in Figure 6 with the simulated data. In particular, data obtained during JONSWAP-75 over growing, reasonably fully developed seas show the same dependence on wind speed as is seen in Figure 6.

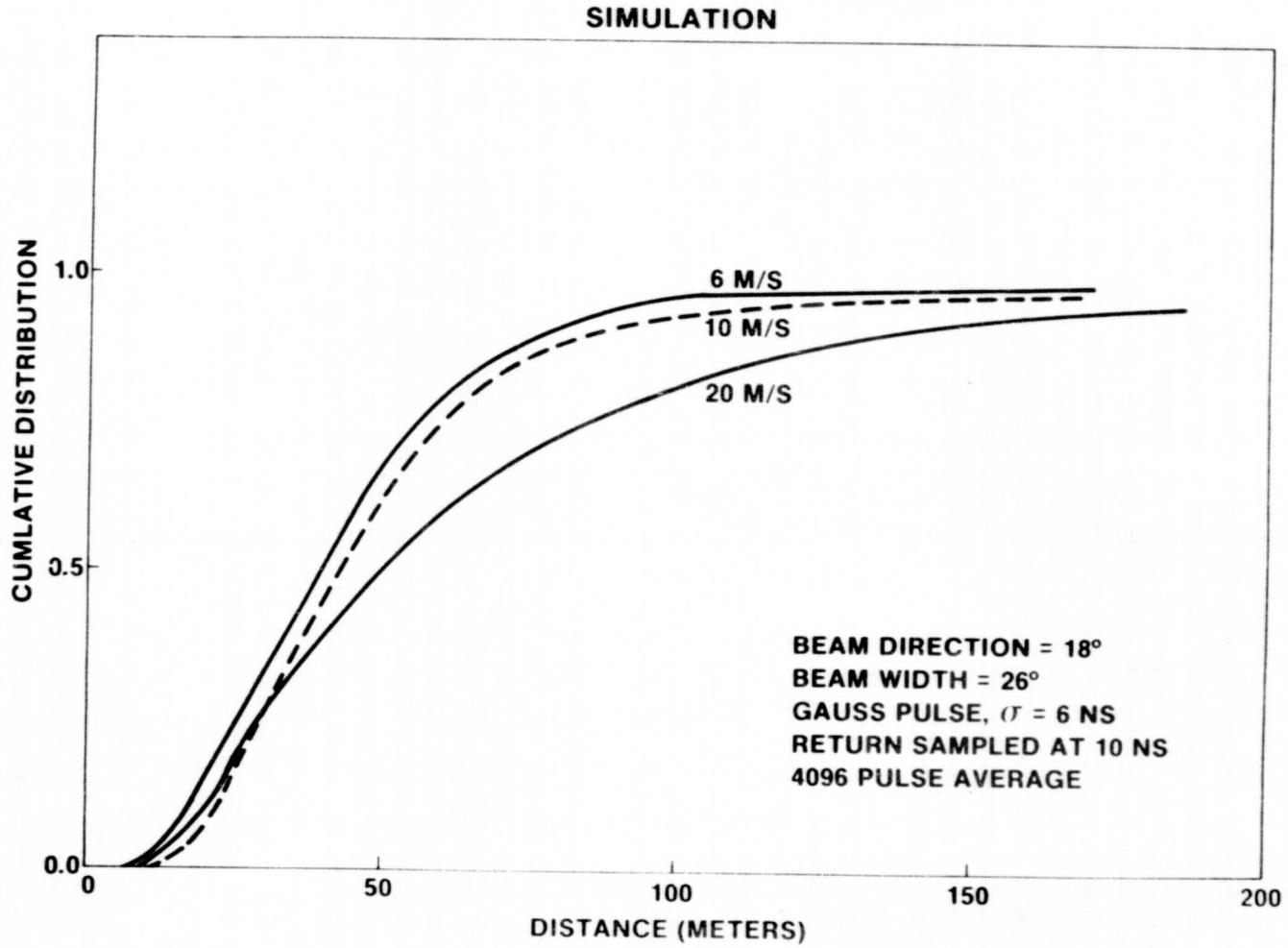

Figure 6. Cumulative distribution of time intervals between peaks in the scatter by a single pulse. These curves represent simulated data using surfaces corresponding to wind speeds of 6, 10, and 20 M/s.

During JONSWAP-75 the GSFC radar was mounted aboard a C-130 aircraft and flown in several different straight line and circular paths over an instrumented piece of ocean near the coat of West Germany (Le Vine, et al., 1977). The relevant ocean truth consisted of wave rider stations and an instrumented tower ("Pisa") at which wave and wind measurements were made. During the period from the morning of September 9, 1975 through the morning of the following day, a period of growing seas, three nearly identical flights were made over Pisa. The path followed on each flight is shown in Figure 7 superimposed on the wave-rider network which was employed during the experiment. Each flight was from northwest toward the southeast and passed very close to the tower. Data was collected with a horizontally polarized stick antenna pointing at 18° from the normal and looking perpendicular to the aircraft in the direction of the coast as the plane flew down the line in the direction of the arrow. The aircraft altitude was about 2 km on each flight.

There were three flights along this path between September 9 and 10. They occurred on the morning of September 9, on the afternoon of the same day, and on the morning of September 10. The available wave and wind information for this period indicates it was a period of growing seas so that the three flights should be over successively higher seas. The waverider derived wave spectra indicate reasonably fully developed seas for this period, and wind information obtained at Pisa give winds of about 10 m/s for this period.

The cumulative distribution for intervals between peaks obtained from these flights is plotted in Figure 8. One would expect, based on the results of the simulated data, to see a shift toward longer intervals on the three flights. That is, if the seas had been successively higher with each flight, the cumulative distribution for the flight on the afternoon of September 9 should lie below the curve obtained using data from the flight on the morning of September 9; and the cumulative distribution pertaining to the morning flight on September 10 would be below both. Notice that this general pattern is reflected in the data. The cumulative distribution obtained with data from the September 10 (a.m.) flight suggests higher seas than either of the September 9 flights; and with the exception of the long interval tail, the data for the afternoon of September 9 indicates higher seas than does the morning data.

These results are encouraging, both as regards the simulation as a tool for analyzing radar performance in a near nadir scattering configuration, and as regards the possibility of using pulse interval statistics for monitoring the surface. However, these results represent only one case, and many questions remain. In particular, the results depend on the assumption of fully developed seas and do not take into account effects of radar orientation with respect to wave direction. Work is presently underway to address these issues, both by

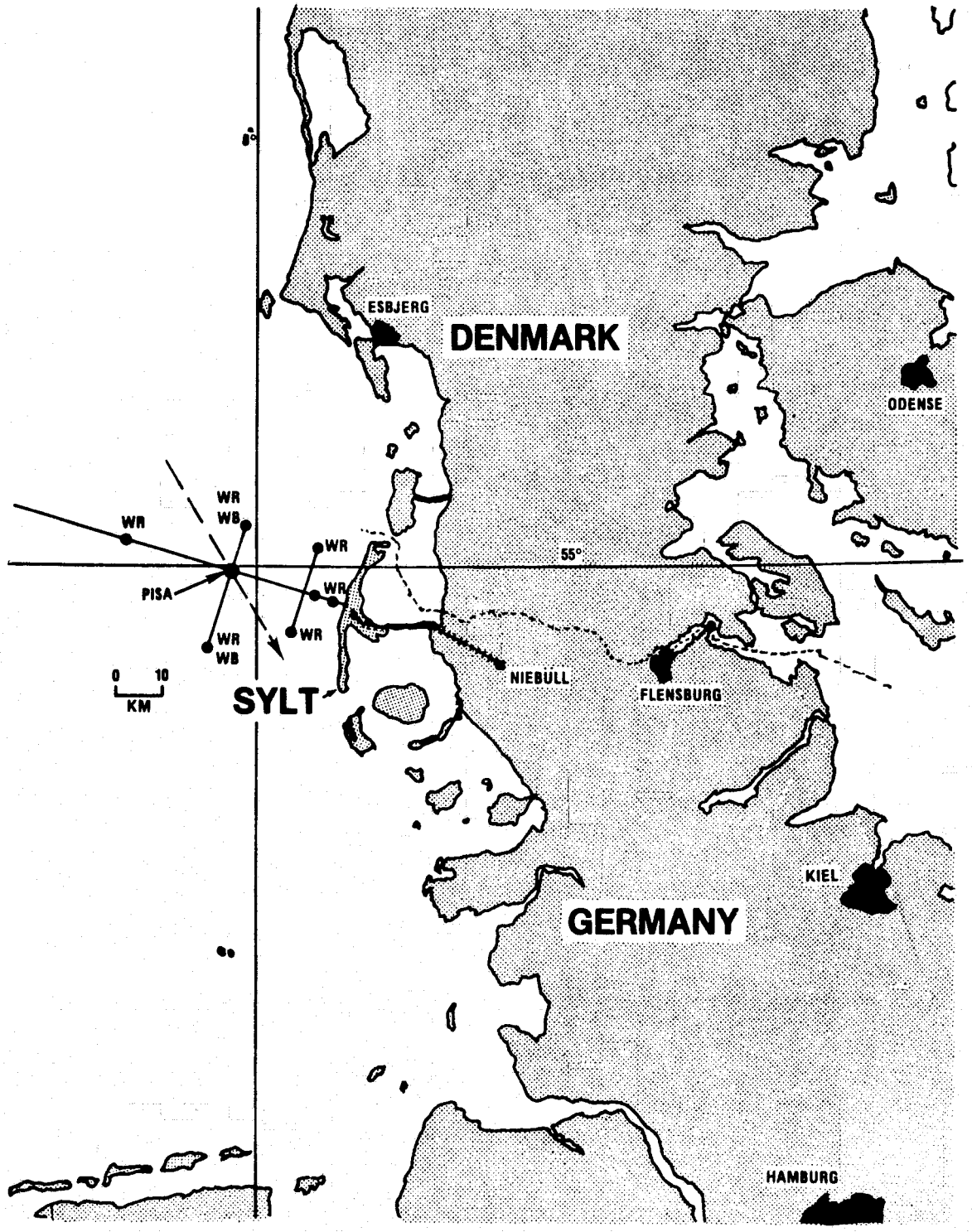

Figure 7. Flight Line Along Which Data was Collected During JONSWAP-75

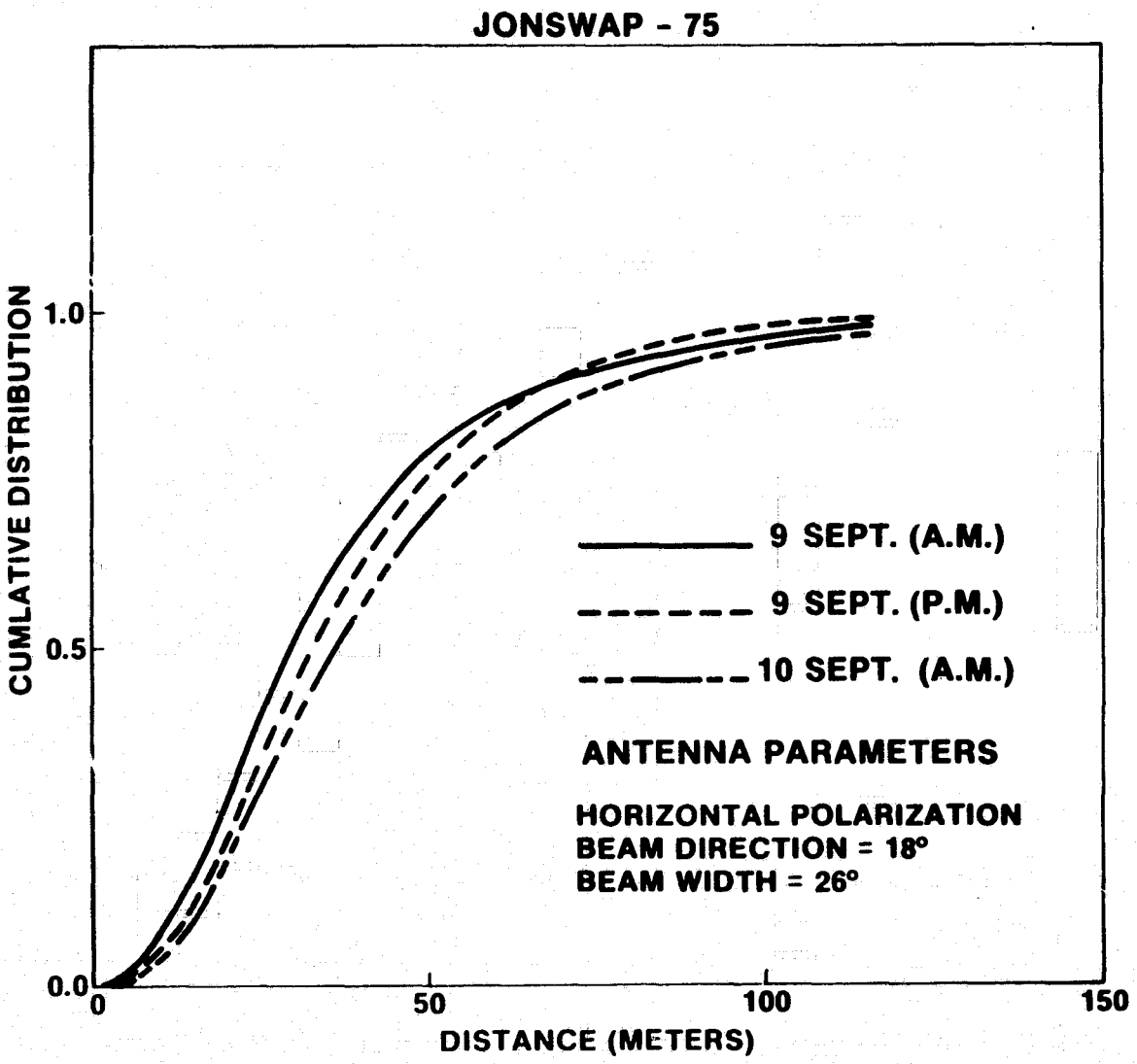

Figure 8. Cumulative Distribution of Interval Between Peaks Using Data Obtained During JONSWAP-75

improving the simulation and by comparing with the data obtained with the GSFC short pulse radar during JONSWAP-75 and also during several subsequent flights aboard the NASA CV-990.

ACKNOWLEDGMENT

The JONSWAP surface truth were courtesy of Klaus Hasselman and his staff at the Max-Planck-Institute für Meterologie (waverider spectra) and Linwood Jones of NASA/LaRc (wind estimates). The GSFC participation in JONSWAP-75 would not have been possible without the hard work of W. T. Walton and M. Dombrowski and others on the radar team at GSFC.

REFERENCES

Barrick, D. E., (1972), "Remote Sensing of the Sea State by Radar," Chapter 12, Remote Sensing of the Troposphere, V. E. Derr, Ed., U.S. Govt. Printing Office.

Barrick, D. E. and W. H. Peake, (1968), "A review of scattering from surfaces with different roughness scales," Radio Science 3, pp. 865-868.

Bass, F. G., et al., (1968), "Very High Frequency Radiowave Scattering by a Distrubed Sea Surface," IEEE Trans. AP-16 (5), pp. 554-568.

Harger, R. O. and D. M. Le Vine, (1976), "Microwave Scatter and Sea State Estimation: Two-Scale Ocean Wave Models," Presented at IUCRM Colloquium on Radio Oceanography, Hamburg, West Germany, September 29 - October 6, To be published in Brendom Foyer Meteorology. (Also see NASA X-952-75-28 September 1975).

Le Vine, D. M., (1974), "Spectrum of Power Scattered by a Short Pulse from a Stochastic Surface," NASA X-952-74-299, April.

Le Vine, D. M., et al., (1977), "GSFC Short Pulse Radar, JONSWAP-75," NASA TN D-8502, June.

Pierson, W. J. and L. Moskowitz, (1964), "A proposed spectral form for fully developed seas based on the similarity theory of S. A. Kitaigorodskii," J. Geophys. Res., 69(24), pp. 5181-5190.